Tutte's Barycenter Method applied to Isotopies ⋆

Éric Colin de Verdière *

Laboratoire d'informatique de l'École normale supérieure, UMR 8548 (CNRS), Paris, France

Michel Pocchiola

Laboratoire d'informatique de l'École normale supérieure, UMR 8548 (CNRS), Paris, France

Gert Vegter

Department of Mathematics and Computer Science, University of Groningen, The Netherlands

Abstract

This paper is concerned with applications of Tutte's barycentric embedding theorem (Proc. London Math. Soc. 13 (1963), 743–768). It presents a method for building isotopies of triangulations in the plane, based on Tutte's theorem and the computation of equilibrium stresses of graphs by Maxwell–Cremona's theorem; it also provides a counterexample showing that the analogue of Tutte's theorem in dimension 3 is false.

Key words: Barycentric embedding theorem, planar graph, triangulation, isotopy, Maxwell–Cremona correspondence, simplicial complex
1991 MSC: 57Q37
1991 MSC: 05C10

This paper appeared in *Computational Geometry: Theory and Applications*, 26 (2003), 81–97.

1 Introduction

1.1 Background on Tutte's barycenter theorem

In this paper, we will use basic graph theory terminology, see for example [6]. Let $G = (V, E)$ be a planar graph. A *mapping* Γ of G into the plane is a function $\Gamma : V \cup E \to \mathcal{P}(\mathbb{R}^2)$ which maps a vertex $v \in V$ to a point in $\mathbb{R}^2$ and an edge $e = uv \in E$ to the straight line segment joining $\Gamma(u)$ and $\Gamma(v)$. A mapping is an *embedding* if distinct vertices are mapped to distinct points, and the open segment of each edge does not intersect any other open segment of an edge or a vertex.

In 1963, Tutte [40] gave a way to build embeddings of any planar, 3-connected graph $G = (V, E)$. Let C be a cycle whose vertices are the vertices of a face of G in some (not necessarily straight-line) embedding of G. Let Γ be a mapping of G into the plane, satisfying the conditions:

- the set V_e of the vertices of the cycle C is mapped to the vertices of a strictly convex polygon Q, in such a way that the order of the points is respected;
- each vertex in $V_i = V \setminus V_e$ is a barycenter with positive coefficients of its adjacent vertices (Tutte assumed all coefficients to be equal to 1, but the proof extends without changes to this case). In other words, the images $\overline{v}$ of the vertices v under Γ are obtained by solving a linear system (S): for each $u \in V_i$, $\sum_{v|uv\in E} \lambda_{uv}(\overline{u} - \overline{v}) = 0$, where the λ_{uv} are positive reals. It can be shown that the system (S) admits a unique solution, see Appendix A.

Theorem 1 (Tutte's Theorem) *Γ is an embedding of G into the plane, with strictly convex interior faces.*

In his paper [40], in addition to showing Theorem 1, Tutte simultaneously proves again Kuratowski's planarity criterion [28] of 1930: a graph is planar unless it contains a subdivision of one of the two Kuratowski graphs K_5 and $K_{3,3}$. The proofs of both results are entangled together in Tutte's paper; the

⋆ This work was initiated while the third author was visiting École normale supérieure. Part of it is the D.E.A. of the first author [13], mainly done at the University of Groningen; this author was partly supported by the Action de recherche coopérative "Visibilité tridimensionnelle : théorie et applications" of Inria.
∗ Corresponding author.
Email addresses: Eric.Colin.de.Verdiere@ens.fr (Éric Colin de Verdière), Michel.Pocchiola@ens.fr (Michel Pocchiola), gert@cs.rug.nl (Gert Vegter).
URLs: http://www.di.ens.fr/~colin/ (Éric Colin de Verdière), http://www.di.ens.fr/~pocchiol/ (Michel Pocchiola), http://www.cs.rug.nl/~gert/ (Gert Vegter).

consequence is that proving Theorem 1 by his method is long and involves quite a lot of graph theory terminology. Later, short proofs of Kuratowski's criterion were given by Thomassen [38], making Tutte's graph-theoretic viewpoint less attractive for the proof of Theorem 1.

Other proofs of this theorem exist in the literature, using a more geometric viewpoint. Becker and Hotz [1] use the notion of "quasi-planarity" as the limit case of a planar situation, which yields complicated notations and tedious case analyses; the structure of their paper is non-obvious and the proof is really long. Y. Colin de Verdière [14] shows the result, only for triangulated graphs, on arbitrary surfaces of non-positive curvature using the Gauss-Bonnet formula. More recently, in 1996, Richter-Gebert [32, Section 12.2] has given a simple and transparent proof of this theorem. [1]

The history of graph embeddings began early. Fáry [19], Stein [37] and Wagner [42] independantly showed that any planar graph admits a (straight-line) embedding. Now, the literature on this subject is abundant; a survey on graph drawing is [15]. See also the books by Ziegler [45] and Richter-Gebert [32] for the important connection between graphs and polytopes by Steinitz' theorem (any 3-connected, planar graph can be realized as the 1-skeleton of a 3D polytope).

Embeddings are not the only way to represent graphs; among others, an alternative approach is to represent the graph with a set of non-overlapping disks in the plane, one for each vertex, so that two vertices are adjacent if and only if the corresponding disks are tangent. This approach is called *circle packing* [33,7].

Recent works also focus on finding embeddings of graphs so that the coordinates of the vertices are integers with absolute value as small as possible; there is a linear algorithm [12] to embed graphs with $n+2$ vertices on the $(n \times n)$-grid with convex faces. Tutte's method with unit coefficients is not a valuable method for this purpose, since it can yield embeddings with exponential area if all coordinates are integers [16]. Any 3-connected planar graph with $n+1$ faces can be embedded on the $(n \times n)$-grid [20]. Other criteria are also interesting, such as controlling the shapes of the faces and/or minimizing the area of the embedding if a minimum distance between two vertices, or between a vertex and a non-incident edge, is imposed [11]. Another topic of interest is also to have an effective version of Steinitz' theorem. This can be done on the cubic grid of size 2^{13n^2}, where n is the number of vertices of the

[1] We have independantly discovered in 2000 a proof of Tutte's theorem, very similar to Richter-Gebert's proof, without being aware of its existence. This proof is available in the electronic proceedings of the 13th Canadian Conference on Computational Geometry at `http://compgeo.math.uwaterloo.ca/~cccg01/proceedings/long/colin-41348.ps.gz`.

graph [32, p. 143].

Tutte's method is the cornerstone of *Floater's parameterization technique* [21] for surface parameterization in computer graphics, used in multiresolution problems [17], texture mapping [29], and morphing [27,22,24].

1.2 Our work

1.2.1 Isotopies

Tutte's theorem yields a method, described by Floater and Gotsman [22] and Gotsman and Surazhsky [24], to morph two triangulations, the boundary being the same convex polygon in both embeddings. One can compute coefficients $\lambda_{uv} > 0$, for each interior vertex u and each neighbor v of u, so that u is the barycenter with coefficients $(\lambda_{uv})_v$ of its neighbors in the initial embedding. Doing the same for the final embedding and interpolating linearly the coefficients yields an isotopy (a continuous family of embeddings) by Tutte's theorem. This method leaves some freedom for the computation of the barycentric coefficients of the vertices in both embeddings. Hence, we study the following natural question: is it possible to apply the same technique, with the additional restriction that the coefficients are symmetric ($\lambda_{uv} = \lambda_{vu}$)? The interest is that this has a clear and appealing physical interpretation: fix the exterior vertices and edges and replace each interior edge joining two vertices u and v by a spring with rigidity λ_{uv}; then the equilibrium state of this physical system is the solution of the system (S). The problem of computing such symmetric coefficients is solved with Maxwell–Cremona's theorem from rigidity theory. The drawback of our method is that these coefficients are not always positive, hence Tutte's theorem does not apply in all cases. After small experiments (with 20 vertices or so), we thought that our method always yielded an isotopy, even if some weights were negative. This is not the case, and we have small examples refuting this conjecture. However, our method gives positive coefficients if both embeddings are in the rather general class of regular triangulations (recall that a regular subdivision is the projection of the lower faces of a polytope generated by a family of points). This idea of replacing edges of a graph by springs has been used in several other contexts: in mechanics [43], for graph connectivity computation [30], in an algorithmic study of operations on polyhedra [26]. Force-directed algorithms (see [15]) are an important class of graph drawing methods that use springs (with, additionally, electric and/or magnetic forces). In [23] is described a tool for the visualization of evolving embeddings of graphs.

1.2.2 Generalization to 3D space

The other main part of this paper is devoted to the study of the extension of Tutte's theorem to three dimensions. It presents an overview of the proof that there exist two triangulations of a tetrahedron which are combinatorially equivalent but for which there is yet no linear isotopy from one to the other, a fact which is specific to spaces of dimension ≥ 3. This result has been stated by Starbird in [34]; we give an outline of the proof and explain parts of the proof not written in his paper and required to show this theorem. Then we show that the natural generalization of Tutte's barycentric embedding theorem is false in 3D. The translation of Tutte's hypotheses (in the triangulated case) from 2D to 3D is as follows: consider an embedding of a simplicial 3-complex K into $\mathbb{R}^3$, the boundary being a convex polyhedron. If a mapping of K into $\mathbb{R}^3$, with the same boundary, is so that each interior vertex is barycenter with positive coefficients of its neighbors, then we would expect that it is an embedding. It turns out that this fact is false. To our knowledge, this attempt of generalizing Tutte's theorem for 3D complexes is new, and our refutation of this extension raises interesting open questions, in the context of isotopies as well as in view of embedding 3-complexes.

2 Isotopies in the plane

Now, we detail the construction of the isotopy outlined in the introduction. Let $G = (V, E)$ be a 3-connected planar graph, and let Γ_0 and Γ_1 be two embeddings of G into the plane. We look for an isotopy between Γ_0 and Γ_1, restricting ourselves to the following situation: the boundary cycle C of the exterior face of Γ_0 is a convex polygon, it bounds also the exterior face of Γ_1, and the corresponding vertices of C are at the same location in Γ_0 and Γ_1. During the isotopy, the vertices of C have to remain at the same position. In addition, we will require the graph G to be triangulated. See Figure 1.

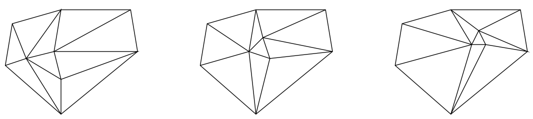

Fig. 1. An isotopy Γ_t ($t \in [0, 1]$) in our framework: here Γ_0, $\Gamma_{1/2}$ and Γ_1 are depicted.

A natural idea arising to solve this problem is the following: try to deform Γ_0 into Γ_1 by keeping the exterior vertices at the same place and moving the interior vertices linearly. That is, $\Gamma_t(v) = (1-t)\Gamma_0(v) + t\Gamma_1(v)$ for an interior vertex v and t in $[0, 1]$. It turns out that this approach does not always yield an isotopy, as Figure 2 demonstrates. Bing and Starbird [3], generalizing a result by Cairns [9], showed the existence of an isotopy in the context described above; if the cells are strictly convex, one can ensure that they remain

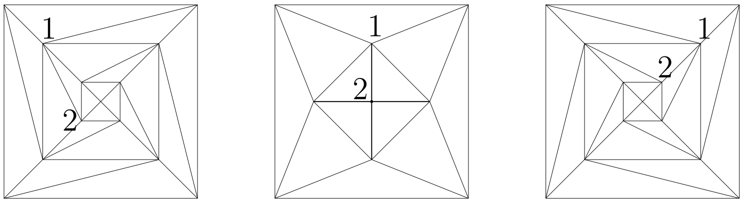

Fig. 2. An example showing that the naive approach does not work. The figure shows Γ_0 (left) and Γ_1 (right). The two inner squares are "twisted" to the left (resp. right) under Γ_0 (resp. Γ_1), and the innermost square must rotate by an angle of π in the whole motion. With the linear motion, the vertices of the inner square would collapse at $t = 1/2$, as shown in the picture in the middle. Therefore, this motion does not yield an isotopy.

strictly convex during the deformation [39]. A series of more mathematical papers study the topological space of embeddings of a given triangulation (with boundary fixed), also called the set of homeomorphisms of a (2D) simplicial complex K that are affine linear on each simplex of K and are the identity on the boundary of K: in [4], it is proved that (if the outer boundary is convex) it is homeomorphic to $\mathbb{R}^{2k}$ where k is the number of interior vertices. See also the references in that paper for further reading on this topic.

However, these papers do not provide an algorithmic solution to this problem. As explained in the introduction, Gotsman et al. [22,24] gave a method, based on Tutte's theorem, to solve this isotopy problem, representing a vertex as barycenter of its neighbors. We will use the following definitions in order to study the case where the barycentric coefficients are symmetric. Let E_i be the set of (undirected) interior edges (the edges for which at least one incident vertex is in V_i). A *weight function* on Γ, or *stress*, is a map $\omega : E_i \to \mathbb{R}$; hence $\omega_{uv} = \omega_{vu}$. ω is *positive* if $\omega_{uv} > 0$ for each interior edge uv. If ω and the positions of each $v \in V_e$ are fixed, the *equilibrium state* is defined by the system: for each $u \in V_i$, $\sum_{v|uv\in E} \omega_{uv}(\overline{u} - \overline{v}) = 0$. In these conditions, ω is an *equilibrium stress* for Γ.

Here is a summary of our approach: compute equilibrium stresses ω^0 (resp. ω^1) of embeddings Γ_0 (resp. Γ_1); then, for $t \in [0, 1]$, compute the equilibrium state of $\omega^t = (1 - t)\omega^0 + t\omega^1$. The difficulty resides in computing an equilibrium stress for a given embedding Γ: our method relies on Maxwell–Cremona's correspondence, a theorem well-known in rigidity theory (see Hopcroft and Kahn [26] for details on this theorem, and [25] for a general introduction to rigidity theory). Think of Γ as being in the plane $z = 0$ of $\mathbb{R}^3$. Take any *lift* of Γ, by adding to each vertex $\bar{v} = p_v = (x_v, y_v, 0)$ of Γ a third coordinate, leading to $q_v = (x_v, y_v, z_v)$. Consider the polyhedral terrain whose vertices are the q_i's and which has the same incidence structure as Γ (Figure 3). Now, let ij be an interior edge of Γ; let l and r be the left and right neighbor of the (oriented) edge ij (Figure 4) and φ^L_{ij} (resp. φ^R_{ij}) the affine form which takes the value z_i, z_j, z_l (resp. z_r) at points p_i, p_j, p_l (resp. p_r). We will define an

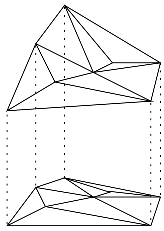

Fig. 3. A lift of an embedding.

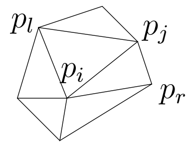

Fig. 4. The notations for the computation of ω_{ij}.

equilibrium stress for Γ determined by this lift.

If $a_0, \ldots, a_k$ are $k+1$ points of $\mathbb{R}^k$, written as column vectors, we introduce the multi-affine bracket operator $[a_0, \ldots, a_k]$, defined by

$$[a_0, \ldots, a_k] = \begin{vmatrix} a_0 & a_1 & \ldots & a_k \\ 1 & 1 & \ldots & 1 \end{vmatrix}$$

(this quantity being proportional to the signed volume of the convex hull of the a_i's).

Lemma 2 *For each interior edge ij and any $p \in \mathbb{R}^2$,*

$$\varphi_{ij}^L(p) - \varphi_{ij}^R(p) = \frac{[p_i, p_j, p]}{[p_i, p_j, p_l]}(\varphi_{ij}^L(p_l) - \varphi_{ij}^R(p_l)).$$

Proof. It is a consequence of Cramer's formula. Let φ be an affine form on $\mathbb{R}^k$ and $a_0, \ldots, a_k$ be $k+1$ affinely independent points, $a \in \mathbb{R}^k$. Let $\alpha_0, \ldots, \alpha_k$ be the barycentric coordinates of a with respect to the a_i's, that is, by definition:

$$\begin{aligned} \alpha_0 a_0 + \ldots + \alpha_k a_k &= a \\ \alpha_0 + \ldots + \alpha_k &= 1. \end{aligned}$$

Cramer's formula now implies:

$$\alpha_i = \frac{[a_0, \ldots, a_{i-1}, a, a_{i+1}, \ldots, a_k]}{[a_0, \ldots, a_k]}.$$

So (if $k = 2$, and because φ is an affine form):

$$\varphi(a) = \frac{[a, a_1, a_2]}{[a_0, a_1, a_2]}\varphi(a_0) + \frac{[a_0, a, a_2]}{[a_0, a_1, a_2]}\varphi(a_1) + \frac{[a_0, a_1, a]}{[a_0, a_1, a_2]}\varphi(a_2).$$

It is now easy to conclude. □

Define, for any interior edge ij and for a point p not on the line $(p_i p_j)$:

$$\omega_{ij} = \frac{\varphi^L_{ij}(p) - \varphi^R_{ij}(p)}{[p_i, p_j, p]}.$$

This definition does not depend on the point p, by Lemma 2. Furthermore, $\omega_{ij} = \omega_{ji}$. In practice, there is an intrinsic formula (recall that the q_i's are the lifts of the points p_i's, which are the images of the vertices under Γ):

Lemma 3 $\omega_{ij} = \dfrac{[q_i, q_j, q_l, q_r]}{[p_i, p_j, p_l][p_i, p_j, p_r]}.$

Proof. By definition of ω_{ij}:

$$\omega_{ij}[p_i, p_j, p_l][p_i, p_j, p_r] = (z_l - \varphi^R_{ij}(p_l))[p_i, p_j, p_r]. \tag{1}$$

By Cramer's formula, as in the proof of Lemma 2:

$$\varphi^R_{ij}(p_l)[p_i, p_j, p_r] = z_i[p_l, p_j, p_r] + z_j[p_i, p_l, p_r] + z_r[p_i, p_j, p_l].$$

Thus the left member of Equation (1) equals

$$z_l[p_i, p_j, p_r] - z_i[p_l, p_j, p_r] - z_j[p_i, p_l, p_r] - z_r[p_i, p_j, p_l],$$

which equals $[q_i, q_j, q_l, q_r]$ (by developping this determinant with respect to the third line). □

Theorem 4 *ω is an equilibrium stress for Γ.*

Proof. For any point p in the plane, $i \in V_i$, we have:

$$\sum_{j|ij\in E} \omega_{ij}[p_i, p_j, p] = \sum_{j|ij\in E} (\varphi^L_{ij}(p) - \varphi^R_{ij}(p)) = 0,$$

because the affine form φ corresponding to a face incident to p_i appears twice in this sum, once counted positively, once negatively. As $[p_i, p_j, p] = \det(p_j - p_i, p - p_i)$, this implies

$$\det\Big(\sum_{j|ij\in E} \omega_{ij}(p_i - p_j), p - p_i\Big) = 0,$$

for each point p in $\mathbb{R}^2$. Therefore

$$\sum_{j|ij\in E} \omega_{ij}(p_i - p_j) = 0.$$

□

Thus, each lift of the embedding Γ determines an equilibrium stress on Γ. Conversely, it is possible to show that an equilibrium stress determines a unique lift of Γ, up to the choice of an affine form of $\mathbb{R}^2$ (Maxwell's theorem, shown for example in [26] in a slightly different context).

If we have *positive* equilibrium stresses ω^0 and ω^1 of Γ_0 and Γ_1 respectively, we have a method to compute an isotopy between Γ_0 and Γ_1: by Tutte's theorem, because $\omega^t = (1-t)\omega^0 + t\omega^1$ is a positive stress for each $t \in [0, 1]$, the corresponding mapping Γ_t is an embedding, and $(\Gamma_t)_{t\in[0,1]}$ is clearly continuous (the map which associates to each invertible matrix its inverse, is continuous), hence an isotopy. Furthermore, it is easy to characterize the set of embeddings which admit a positive equilibrium stress: an edge ij has a positive weight if and only if the line q_iq_j (with the notations above) is under the line q_lq_r. Recall that a *regular triangulation* is a triangulation which is the projection of the lower faces of a polytope generated by a family of points, see [45]. Hence an embedding has a positive stress if and only if it is a regular triangulation. Therefore, we have:

Theorem 5 *If Γ_0 and Γ_1 are regular triangulations, then we can compute an isotopy between Γ_0 and Γ_1.*

Testing whether Γ is a regular subdivision, and, if so, computing a positive lift, can be done easily using linear programming; indeed, we have a convex lift for Γ if and only if, for each interior edge ij and with the notations above, $[q_i, q_j, q_l, q_r] < 0$, which is a linear inequality in the z_k's. Not all triangulations are regular subdivisions, as shown in Figure 5 (see [45, p. 132]), but a large class of embeddings are regular subdivisions, including Delaunay triangulations for example (because the Delaunay triangulation of a set of points is the projection of the edges of the convex hull of the points lifted on the standard paraboloid, see [5, p. 437] or [18, p. 303]); this remark might be useful because of the wide use of these triangulations in computational geometry.

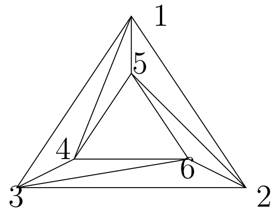

Fig. 5. An embedding which is not a regular subdivision. Indeed, assuming it is possible to lift it to a lower convex hull, we can suppose, by adding a suitable affine form to all the z_i's, that $z_4 = z_5 = z_6 = 0$. If this graph were a regular subdivision, we would have $z_1 > z_2 > z_3 > z_1$, which is impossible.

Remark. We only studied triangulated graphs in this section because it is probably easier to deal with them than with general planar 3-connected graphs. However, the same theory applies if the graph is only 3-connected. The definition of a lift must be adapted: all the vertices belonging to the same face must be lifted on a common plane in 3D space (it also corresponds to triangulating the graph and putting a weight equal to zero on these new edges); testing whether we have a regular subdivision is also a linear programming problem.

In practice, we tried to build an isotopy between a random triangulated embedding and the "canonical" embedding of the same graph (that is, the embedding obtained by Tutte's method when all weights equal 1). We lift Γ_0 to the standard paraboloid $z = x^2 + y^2$, compute the equilibrium stress ω_0, and use linear interpolation between ω^0 and the unit weights ω^1. Although the initial stress is not necessarily positive, it turns out that, in many (not too big) cases, this method yields an isotopy; long experiments have been necessary to find a small counterexample like Figure 6. See Appendix B for numerical coordinates. Our smallest counterexample uses 4 outer vertices and 2 inner vertices, but the failure is very hard to see on the screen and can only be proved by computation. Lifting on the paraboloid may give an isotopy even if the considered triangulation is non-regular, like in Figure 2, but can also fail with regular triangulations (the initial and final triangulations in Figure 6 are regular). This method has been programmed in C++ using Numerical Recipes and the LEDA library, and also in Mathematica for exact computations.

Several other approaches could be done in the same spirit to try to find a method which would work for a larger class of embeddings than the regular subdivisions. One could attempt to study the space of stresses which yield an embedding (thus an isotopy corresponds to a path in this space). If we restrict ourselves to the linear interpolation between the weights, an important question is: are there two embeddings Γ_0 and Γ_1 so that, for any lifts of Γ_0 and Γ_1, the interpolation $\omega^t = (1-t)\omega^0 + t\omega^1$ of the corresponding weights does not yield an isotopy? If it is not the case, how to compute the lifts?

We have seen that using linear interpolation from the weights of a lift on the

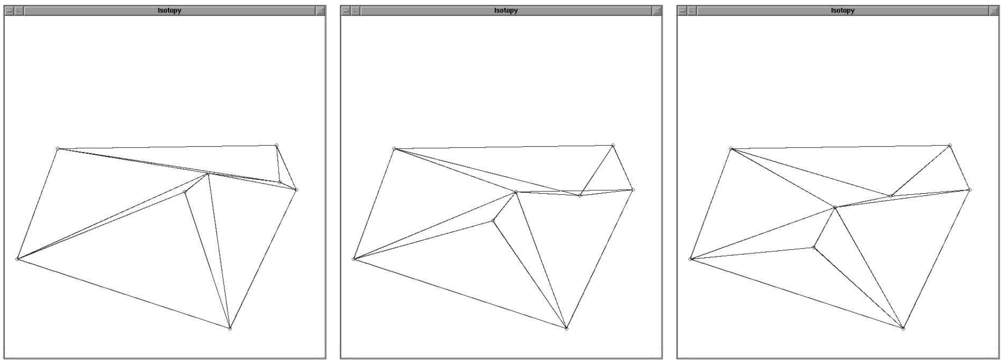

Fig. 6. An example of non-planarity with the linear interpolation between the weights of a lift on the standard paraboloid, and unit weights.

standard paraboloid to unit weights does not always yield an isotopy. Nevertheless, we have the following conjecture (checked during all our experiments): during this interpolation, the matrix involved in the computation of the positions of the points is symmetric positive definite.

If it is the case, it has the following interesting consequence. If ω is a stress on G, let us denote by M_ω the matrix involved in the inversion of System (S). It can be shown (see the proofs of Lemma 9) that M_ω is symmetric positive definite if ω is positive; moreover, $\omega \mapsto M_\omega$ is linear. If M_{ω^0} and M_{ω^1} are symmetric positive definite, so is $M_{(1-t)\omega^0+t\omega^1} = (1-t)M_{\omega^0}+tM_{\omega^1}$, and uniqueness of the positions of the vertices is guaranteed during the motion (which may fail to be an isotopy). Similarly, if M_{ω^0} is symmetric positive definite and ω^1 is a positive stress, since multiplying ω^1 by a positive number does not affect the equilibrium state, we can assume $\omega^1 \geq \omega^0$ (this notation simply means that for each interior edge ij, $\omega^1_{ij} \geq \omega^0_{ij}$). Each nondecreasing family ω^t of stresses from ω^0 to ω^1 yields a family M_{ω^t} of symmetric positive definite matrices; indeed, $M_{\omega^t} = M_{\omega^0} + M_{\omega^t-\omega^0}$; the first matrix of the right term is symmetric positive definite, the second one is positive because the corresponding stress is nonnegative on each interior edge. Thus, if this conjecture is true, the positions of the vertices are uniquely determined for many choices of the interpolation between the weights.

3 Generalization to 3D space

We explain here why the analogue of Tutte's theorem is false in 3D space, thus making it difficult to build isotopies in 3D. Here, it is convenient to use combinatorial simplicial complexes (all simplicial complexes considered here are combinatorial, not geometric; see for example [41]).

We introduce some other definitions, generalizing those in 2D. A *mapping* f from a simplicial complex C into $\mathbb{R}^d$ is a map from all the simplexes of C into $\mathcal{P}(\mathbb{R}^d)$ satisfying: if $\{v_1, \ldots, v_p\}$ is a simplex of C, $f(\{v_1, \ldots, v_p\}) = \mathrm{Conv}\{f(v_1), \ldots, f(v_p)\}$. An *embedding* of C into $\mathbb{R}^d$ is a mapping so that, for any two simplexes $\sigma, \tau \in C$, $f(\sigma \cap \tau) = f(\sigma) \cap f(\tau)$. As usual, an *isotopy* $(h(t))$ $(t \in [0, 1])$ of C into $\mathbb{R}^d$ is a continuous family of embeddings of C into $\mathbb{R}^d$. Finally, the *image* of a simplicial complex C by a mapping f is the union of the sets $f(\tau)$, over all simplexes τ of C.

In this section, we will often manipulate complexes whose embeddings have to be fixed on the "boundary" of these complexes. A *3-complex with tetrahedral boundary* (C, B, b) is a simplicial 3-complex C with a subcomplex $B \subset C$ so that B is simplicially equivalent to the boundary of a 3-simplex, together with an embedding b of B into $\mathbb{R}^3$. An *embedding* f of (C, B, b) into $\mathbb{R}^3$ is an embedding of C so that $f|_B = b$ and the image of f is exactly the tetrahedron bounded by the image of b. An *isotopy* of a 3-complex with tetrahedral boundary is a continuous family of embeddings.

The goal of this section is to show:

Theorem 6 *There exist a complex with tetrahedral boundary (C, B, b), and two mappings f and j of (C, B, b) into $\mathbb{R}^3$, such that:*

(1) f is an embedding,
(2) $j|_B = f|_B$,
(3) each vertex in $C \setminus B$ is, under j, barycenter with positive coefficients of its neighbors,
(4) but j is not an embedding.

This theorem is a counterexample to the analogue of Tutte's theorem in three dimensions: the first condition is the analogue of planarity, the second condition fixes the images of the exterior vertices by j and the third one is the condition for the interior vertices.

The cornerstone for the proof of Theorem 6 is the description by Starbird [34] of a graph C_1, embedded into $\mathbb{R}^3$ in two different ways f_1 and g_1, so that it is impossible to deform one embedding to the other without bending the edges. Yet, if bending the edges is allowed, such a deformation becomes possible. These embeddings are depicted in Figure 7, copied from his paper. We found coordinates for the vertices of these embeddings, available in Appendix C. In the lemma below, we rephrase the properties stated by Starbird.

Lemma 7 *(1) There are a 3-complex with tetrahedral boundary (C, B, b), so that C contains C_1, and two embeddings f and g of (C, B, b) extending respectively f_1 and g_1.*
(2) If C, f and g satisfy the preceding condition, there is no isotopy of

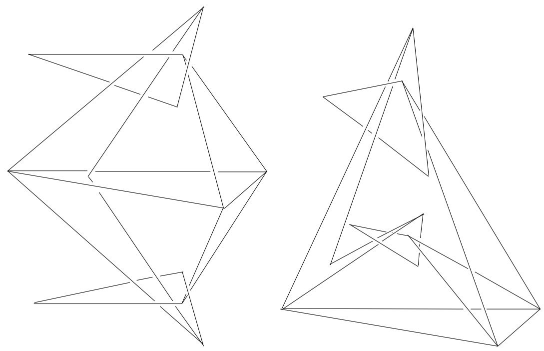

Fig. 7. Starbird's embeddings f_1 and g_1 of C_1.

(C, B, b) *taking* f *to* g*.*

The first part of Lemma 7 expresses the fact that f and g are combinatorially equivalent triangulations (tetrahedralizations for purists) of a tetrahedron, with the same boundary. Despite this, as stated in the second part, there is no isotopy from f to g. It is to be noted that the analogue of this lemma is false in 2D by Tutte's theorem.

The proof of the second part of this lemma is given in detail in Starbird's paper, we shall not explain the argument here. Shortly said, the author uses properties of piecewise linear curves embedded in 3D space to show that the embeddings f_1 and g_1 cannot be deformed from one to the other while keeping the edges of C_1 straight, for otherwise at some stage of the isotopy there would be a degeneracy which would prevent to have an embedding. Then, because f (resp. g) extends f_1 (resp. g_1), there cannot be any isotopy between those embeddings as well.

We will give a detailed summary of the proof of the first part of Lemma 7, because it is stated in Starbird's paper but not all details of the proof are supplied. The key ingredient for the proof is the following "fundamental extension lemma" enabling to extend an isotopy of a complex to an isotopy of a complex with tetrahedral boundary containing this complex. It is proved in [3, Theorem 3.3]; we rephrase it here for convenience in our framework (it holds in fact in arbitrary dimension):

Lemma 8 *Let* C *be a simplicial 3-complex and* $(h(t))$ *be an isotopy of* C *into* $\mathbb{R}^3$*. Then there are a 3-complex with tetrahedral boundary* $(\tilde{C}, \tilde{B}, \tilde{b})$ *so that* $\tilde{C}$ *contains* C *and an isotopy* $(\tilde{h}(t))$ *of* $(\tilde{C}, \tilde{B}, \tilde{b})$ *into* $\mathbb{R}^3$ *extending* $(h(t))$*.*

We shall not give the proof here. The two key ingredients are that slightly perturbing an embedding still yields an embedding, and the use of refinements of triangulations in $\mathbb{R}^3$.

Proof of Lemma 7, first part. We first express the fact that it is possible

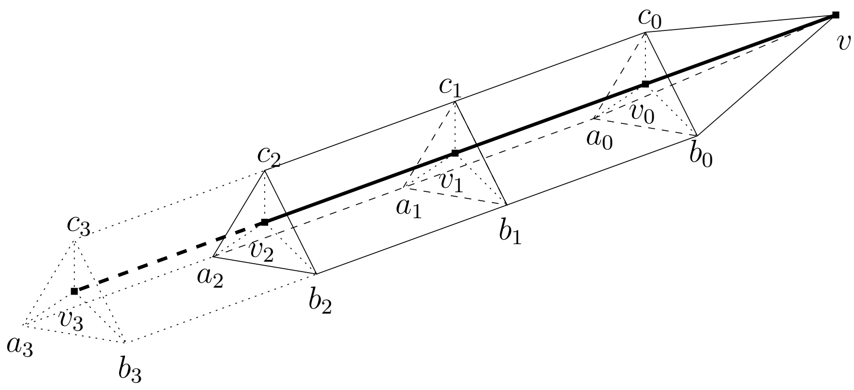

Fig. 8. How an edge vw of C_1 (in bold) is protected by a skinny flexible tube. The vertices $v_0, \ldots, v_n$ are spread uniformly on the edge of C_1 which is considered, to make the edge flexible during the isotopy. An equilateral triangle $a_ib_ic_i$ is drawn around v_i, and the vertices of these triangles are linked as shown in the figure. Note the special treatment at the end of the edge (vertex v). The space between the triangles $a_ib_ic_i$ is also triangulated (not all edges are shown in the figure). Thus, a 3-dimensional simplicial complex protects each edge of C_1.

to deform $f(C_1)$ to $g(C_1)$ if bending the edges is allowed: there is a refinement C_2 of C_1 (by adding vertices on the edges of C_1) and an isotopy $(h(t))$ of C_2 into $\mathbb{R}^3$ taking f_2 to g_2. Here, f_2 is to be understood in the following manner (and similarly for g_2): if v is a vertex in C_1, then $f_2(v) = f_1(v)$; and if an edge $e = vw$ of C_1 is subdivided with vertices $v_0, \ldots, v_n$ inserted on e, then $f_2(v_0), \ldots, f_2(v_n)$ are spread uniformly on $f_1(v)f_1(w)$. It is easy to see that this fact is true, as written in the paper, if you build a model of $f_2(C_2)$ with strings (or small bars) and deform it to $g_2(C_2)$.

No argument apart from the fact that such a deformation is possible is given in Starbird's paper to complete the proof. We thus suggest the following: In fact, we extend a bit more C_2 by protecting each edge of C_1 (split in C_2) by a 3-complex looking like a skinny tube (Figure 8). Define f_2 and g_2 naturally on these tubular protections; the images of f_2 and g_2 are just thickened versions of the images of f_1 and g_1. By Lemma 8, extend C_2 to a 3-complex with tetrahedral boundary (C_3, B_3, b_3), extending the isotopy $(h(t))$ to an isotopy $(\tilde{h}(t))$ of (C_3, B_3, b_3). Now, considering $\tilde{h}(0)$ and $\tilde{h}(1)$, the complex (C_3, B_3, b_3) nearly satisfies the conditions required in the first part of Lemma 7, except that C_3 does not contain exactly C_1 because the edges of C_1 have been subdivided.

Thus, in f_3 and g_3, the only thing we have to do is to retriangulate compatibly the tubular protections of each (split) edge vw of C_1, removing the vertices $v_0, \ldots, v_n$ splitting this edge and restoring the initial edge vw. Since the tubular protections of vw look alike under f_3 and g_3 (the v_i's are on a line, and similarly for the a_i's, b_i's and c_i's), this retriangulation is easy: the compatibility will be automatically satisfied. See [2, p. 4–6] for similar retriangulation problems: first retriangulate the 2D region which is the convex hull of v, w, and the a_i's by removing the v_i's and linking each of the a_i's to v. Do the same with the b_i's and the c_i's. Now, we have to retriangulate three thirds of the tubular protection of edge vw. To retriangulate the region which is the convex hull of v, w, the a_i's and the b_i's, simply insert a new vertex p in the interior of this region; since its boundary is still triangulated, it is sufficient to insert in the complex the simplexes which are on the boundary of this region with p adjoined ("coning" the boundary of this region from p). Do the same for the other thirds. The resulting complex (C, B, b) and embeddings f and g satisfy the hypotheses. □

Proof of Theorem 6. First notice that, under f and g, all interior vertices are barycenter with positive coefficients of their adjacent vertices. For otherwise a vertex i would be on a face of the polytope generated by the neighbors of i, hence i would have no neighbor on a half-space whose boundary passes through the image of i; this contradicts the fact that i is a vertex interior to the triangulation. Let i be an interior vertex, and let λ_{ij}^f (resp. λ_{ij}^g) be the barycentric coefficients of i with respect to its neighbors j in the embedding f (resp. g). Note that the coefficients may be non-symmetric: we follow the approach of [22] to ensure we have positive coefficients. Then, for $t \in [0, 1]$, consider $\lambda_{ij}^t = (1-t)\lambda_{ij}^f + t\lambda_{ij}^g > 0$. Fix the positions p_i of the vertices $i \in B$, and look for the positions of the other vertices i satisfying the equations: $\sum_{j|ij\in E} \lambda_{ij}^t (p_j - p_i) = 0$, where E is the set of edges of C. This system admits a unique solution for each $t \in [0, 1]$ (exactly the same proof holds as in Appendix A). Let us call the resulting family of mappings $(\bar{h}(t))$. By Lemma 7, second part, $(\bar{h}(t))$ cannot be an isotopy: there is a $t_0 \in [0, 1]$ such that $\bar{h}(t_0) = j$ is not an embedding. $(C, B, b), f$, and j satisfy the conditions of Theorem 6. □

This theorem is a counterexample to the generalization of Tutte's theorem in 3D, described in introduction. In fact, the result is slightly stronger: j is not an embedding, but even the restriction of j to the 1-skeleton of C is not an embedding (two edges must cross). This also implies that constructing isotopies of complexes in 3D is much more difficult than in 2D. Starbird [35,36] showed the following theorem which might be a clue to find a solution: if there are two embeddings f and g of a complex K with tetrahedral boundary into $\mathbb{R}^3$ (or more generally if the boundary is a convex polyhedron), then there might be no isotopy from f to g, but there is always a suitable refinement K' of the complex K for which there is an isotopy between f and g. The problem is now to realize algorithmically the refinement and the isotopy; unfortunately, it is unclear how to proceed. Another track would be to try to find more restrictive conditions under which a barycentric method would work; for example, if some subcomplexes are forbidden, or if the complex is sufficiently refined, does Tutte's barycentric method always yield an embedding?

4 Note added in proof

Recently, other counter-examples for the analogue of Tutte's theorem in 3D were found by Ó Dúnlaing (Proc. Europ. Workshop. Comput. Geom 2002 75–79) and Floater and Pham-Trong (Internat. Conf. Curves and Surfaces 2002).

Acknowledgements

We would like to thank Yves Colin de Verdière and Michael Starbird for helpful discussions on their papers, Francis Lazarus for interesting comments, Robert Connelly for references on this topic, and the anonymous referees for providing us references, in particular the book by Richter-Gebert containing his proof of Tutte's theorem.

A Invertibility of System (S)

Lemma 9 *If the coefficients λ_{ij} are positive, System (S) admits a unique solution.*

Before showing this lemma, we must explicitely compute the entries of the matrix involved in System (S). For convenience, note $v_1, \ldots, v_m$ the interior vertices and $v_{m+1}, \ldots, v_n$ the exterior ones. The matrix involved in System (S) is square, of size m, and defined, if $1 \leq i, j \leq m$ and with the convention $\lambda_{ij} = 0$ if ij is not an edge, by:

$$m_{ij} = -\lambda_{ij}, \text{ if } i \neq j;$$

$$m_{ii} = \sum_{k=1}^{n} \lambda_{ik}.$$

Several proofs of this lemma exist in the literature. We first give the most straightforward proof in the general case. It uses the well-known "diagonal dominant property" of matrices and can be found in [21, p. 237].

Proof. We show that the kernel of M is $\{0\}$. If $M \cdot y = 0$ for a column vector y with m entries, then: for each $i \in \{1, \ldots, m\}$, $\sum_{j=1}^{n} \lambda_{ij}(y_i - y_j) = 0$, where $y_j = 0$ if $j > m$ by definition. Consider an index i such that $|y_i|$ is maximal. As λ is positive, the preceding equation yields $y_j = y_i$ for every j neighbor of i. Because G is connected, and because $y_j = 0$ if $j > m$, we get

$y_i = 0$. Therefore, M is invertible. (In fact, the same argument shows that M is symmetric definite positive, for it cannot have a nonpositive eigenvalue.) □

We now prove Lemma 9 in the special case where the coefficients are symmetric, using the physical interpretation with the springs. E_i denotes the set of interior edges.

Proof. The energy of the system made of the springs is defined by $\mathcal{E} = \frac{1}{2}\sum_{ij\in E_i} \lambda_{ij}|p_j - p_i|^2$. Consider that the positions of the exterior vertices are fixed; $\mathcal{E}(p_1, \ldots, p_m)$ is a polynomial function of degree two. If at least one interior vertex p_i goes to infinity, $\mathcal{E}$ tends to $+\infty$ by connectivity of G and positivity of the coefficients. Thus, the homogeneous polynomial of degree two in the coordinates $p_1, \ldots, p_m$ of $\mathcal{E}$ is a quadratic form which is symmetric definite positive. But the matrix of this quadratic form is exactly the matrix M, as it can be checked easily using the fact that the coefficients are symmetric. Thus M is symmetric definite positive and (S) admits a unique solution. □

Finally, we indicate that Lemma 9 is a consequence of the *matrix tree theorem* (see Brualdi and Ryser [8, p. 324], Chaiken [10], Orlin [31] or Zeilberger [44]), a theorem interpreting combinatorially the determinant of certain matrices in terms of arborescences of graphs.

Proof. Let $(n_{ij})_{1\leq i\neq j\leq m+1}$ be real numbers. Consider the complete directed graph (without loops) $\bar{G}$ with $m+1$ vertices, each edge (ij) having, by definition, weight n_{ij}. Let P be the square matrix of size $m+1$ defined by:

$$p_{ij} = -n_{ij}, \text{ if } i \neq j;$$

$$p_{ii} = \sum_{k=1}^{m+1} n_{ik}.$$

The matrix P is called the *Laplacian matrix* of $\bar{G}$. A *spanning arborescence* of $\bar{G}$ rooted at i is a subgraph of $\bar{G}$ covering all vertices of $\bar{G}$ so that it has no directed cycle and all vertices $j \neq i$ have, in $\bar{G}$, outdegree equal to one. The *matrix tree theorem* asserts that the cofactor of the ith diagonal element of matrix P is exactly the sum, over all spanning arborescences of $\bar{G}$ rooted at i, of the product of the weights of the edges of this arborescence.

Apply this theorem to our particular case: let $n_{ij} = \lambda_{ij}$ if $1 \leq i \neq j \leq m$; if $i \leq m$, let $n_{i,m+1} = \sum_{k=m+1}^{n} \lambda_{ik}$ and $n_{m+1,i} = 0$. The $(m+1)$th cofactor of P is exactly the determinant of the matrix M and also equals the sum, over all spanning arborescences of $\bar{G}$ rooted at vertex $m+1$, of the product of the weights of the edges of this arborescence. There is at least one spanning arborescence yielding a nonzero contribution to this sum: to see this, take a spanning tree of the graph induced by the inner vertices of G, and add one directed edge from a vertex in G which, in G, is linked to an exterior vertex, to vertex $m+1$. Since the weights of the edges are nonnegative, the contribution of any spanning arborescence is nonnegative, hence the cofactor is positive and M is invertible. □

B Counter-examples

We present here the data sets of embeddings which present a failure of the method presented in Section 2 (by lifting the embedding on the standard paraboloid to compute the initial weights, and then using linear interpolation between these weights and the unit weights).

The data format is as follows: each line corresponds to a vertex of the embedding, and contains, in this order, the vertex number, its x- and y-coordinates, and the list of its neighbors.

B.1 The smallest counter-example found

In this counter-example, the situation is close to a degeneracy, but one can check by numerical computation that this mapping is indeed an embedding, and that this does not yield an isotopy. It is made of four exterior vertices and two interior vertices.

```
1 -500 900 2 5 6 4
2 -850 900 1 3 5
3 -950 -900 4 6 5 2
4 0 -400 1 6 3
5 -900 -699 6 1 2 3
6 -800 -300 1 5 3 4
```

B.2 Counter-example presented in Figure 6

```
1 -681.67 314.31 5 2 8 6
2 -938.19 -391.67 7 8 1 3
3 419.75 -833.89 4 8 7 2
4 841.39 52.42 5 6 8 3
```

```
5 712.91 332.73 1 6 4
6 733.43 99.34 5 1 8 4
7 128.62 38.94 8 2 3
8 277.47 156.82 1 2 7 3 4 6
```

C Coordinates for Starbird's embeddings

We present here two data sets in OOGL format (to be viewed for example with Geomview[2]), which are Starbird's embeddings presented in Figure 7. The format of the main part of each data set is as follows: each line denotes a vertex, with its x-, y- and z-coordinates. Each pair of lines denotes an edge.

[2] `http://www.geomview.org`

First embedding:

```
VECT

17 34 17
2 2 2 2 2 2 2 2 2 2
2 2 2 2 2 2 2
1 1 1 1 1 1 1 1 1 1
1 1 1 1 1 1 1
####################
# Center part

0   -20 0   # 7
-4  20  0   # 5

-4  20  0   # 5
4   20  0   # 6

4   20  0   # 6
0   -20 0   # 7

# Upper part

4   20  0   # 6
-6  0   16  # '4

-6  0   16  # '4
-16 -6  14  # '3

-16 -6  14  # '3
2   6   8   # '2
```

```
2   6   8   # '2
-10 6   20  # '1

-10 6   20  # '1
0   -20 0   # 7

-10  6  20  # '1
0    -12 0  # 8

-4  20  0   # 5
-6  0   16  # '4

# Lower part (symm.
# in Z of upper part)

4   20  0   # 6
-6  0   -16 # 4

-6  0   -16 # 4
-16 -6  -14 # 3

-16 -6  -14 # 3
2   6   -8  # 2

2   6   -8  # 2
-10 6   -20 # 1

-10 6   -20 # 1
0   -20 0   # 7
```

```
-10  6   -20# 1
0    -12 0  # 8

-4  20  0   # 5
-6  0   -16 # 4
####################
1 0 0 1
1 0 0 1
1 0 0 1
1 0 0 1
1 0 0 1
1 0 0 1
1 0 0 1
1 0 0 1
1 0 0 1
1 0 0 1
1 0 0 1
1 0 0 1
1 0 0 1
1 0 0 1
1 0 0 1
1 0 0 1
1 0 0 1
```

Second embedding:

```
VECT

17 34 17
2 2 2 2 2 2 2 2 2 2
2 2 2 2 2 2 2
1 1 1 1 1 1 1 1 1 1
1 1 1 1 1 1 1
####################
# Center part

0   -20 0   # 7
-4  20  0   # 5

-4  20  0   # 5
4   20  0   # 6

4   20  0   # 6
0   -20 0   # 7

# Upper part

4   20  0   # 6
-6  0   24  # '4

-6  0   24  # '4
-16 -6  21  # '3

-16 -6  21  # '3
2   6   12  # '2
```

```
2   6   12  # '2
-10 6   30  # '1

-10 6   30  # '1
0   -20 0   # 7

-10  6  30  # '1
0    -12 0  # 8

-4  20  0   # 5
-6  0   24  # '4

# Lower part (symm.
# in X, shrink in Z
# of upper part)

-4  20  0   # 6
6   0   8   # 4

6   0   8   # 4
16  -6  7   # 3

16  -6  7   # 3
-2  6   4   # 2

-2  6   4   # 2
10  6   10  # 1

10  6   10  # 1
0   -20 0   # 7
```

```
10   6   10 # 1
0    -12 0  # 8

4   20  0   # 5
6   0   8   # 4
####################
1 0 0 1
1 0 0 1
1 0 0 1
1 0 0 1
1 0 0 1
1 0 0 1
1 0 0 1
1 0 0 1
1 0 0 1
1 0 0 1
1 0 0 1
1 0 0 1
1 0 0 1
1 0 0 1
1 0 0 1
1 0 0 1
1 0 0 1
```

References

[1] B. Becker and G. Hotz. On the optimal layout of planar graphs with fixed boundary. *SIAM Journal on Computing*, 16(5):946–972, 1987.

[2] R. H. Bing. *The geometric topology of 3-manifolds*. American Mathematical Society, 1983.

[3] R. H. Bing and M. Starbird. Linear isotopies in E^2. *Transactions of the American Mathematical Society*, 237:205–222, 1978.

[4] E. D. Bloch, R. Connelly, and D. W. Henderson. The space of simplexwise linear homeomorphisms of a convex 2-disk. *Topology*, 23(2):161–175, 1984.

[5] J.-D. Boissonnat and M. Yvinec. *Algorithmic Geometry.* Cambridge University Press, 1998.

[6] B. Bollobás. *Modern graph theory*, volume 184 of *Graduate Texts in Mathematics*. Springer-Verlag, 1998.

[7] G. R. Brightwell and E. R. Scheinerman. Representations of planar graphs. *SIAM Journal on Discrete Mathematics*, 6(2):214–229, 1993.

[8] R. A. Brualdi and H. J. Ryser. *Combinatorial matrix theory*, volume 39 of *Encyclopedia of Mathematics and its Applications*. Cambridge University Press, 1991.

[9] S. S. Cairns. Deformations of plane rectilinear complexes. *American Mathematical Monthly*, 51:247–252, 1944.

[10] S. Chaiken. A combinatorial proof of the all minors matrix tree theorem. *SIAM Journal on Algebraic and Discrete Methods*, 3:319–329, 1982.

[11] M. Chrobak, M. T. Goodrich, and R. Tamassia. Convex drawings of graphs in two and three dimensions. In *Proceedings of the 12th Annual ACM Symposium on Computational Geometry*, pages 319–328, 1996.

[12] M. Chrobak and G. Kant. Convex grid drawings of 3-connected planar graphs. *International Journal on Computional Geometry and Applications*, 7(3):211–223, 1997.

[13] É. Colin de Verdière. Isotopies de graphes planaires avec applications à la métamorphose. D.E.A., École normale supérieure (Paris), 2000. `http://www.di.ens.fr/~colin/textes/dea.ps.gz`.

[14] Y. Colin de Verdière. Comment rendre géodésique une triangulation d'une surface ? *L'Enseignement Mathématique*, 37:201–212, 1991.

[15] G. Di Battista, P. Eades, R. Tamassia, and I. G. Tollis. *Graph Drawing.* Prentice Hall, 1999.

[16] P. Eades and P. Garvan. Drawing stressed planar graphs in three dimensions. In *Graph drawing (Passau, 1995)*, pages 212–223. Springer, 1996.

[17] M. Eck, T. DeRose, T. Duchamp, H. Hoppe, M. Lounsbery, and W. Stuetzle. Multiresolution analysis of arbitrary meshes. *Computer Graphics*, 29(Annual Conference Series):173–182, 1995.

[18] H. Edelsbrunner. *Algorithms in Combinatorial Geometry*, volume 10 of *EATCS Monographs on Theoretical Computer Science*. Springer-Verlag, 1987.

[19] I. Fáry. On straight line representations of planar graphs. *Acta scientiarum mathematicarum(Szeged)*, 11:229–233, 1948.

[20] S. Felsner. Convex drawings of planar graphs and the order dimension of 3-polytopes. *Order*, 18(1):19–37, 2001.

[21] M. Floater. Parametrization and smooth approximation of surface triangulations. *Computer Aided Geometric Design*, 14(3):231–250, 1997.

[22] M. S. Floater and C. Gotsman. How to morph tilings injectively. *Journal of Computational and Applied Mathematics*, 101:117–129, 1999.

[23] C. Friedrich and P. Eades. The Marey graph animation tool demo. In *Proceedings of the 8th International on Graph Drawing 2000*, volume 1984 of *Lecture Notes in Computer Science*, pages 396–406, 2001.

[24] C. Gotsman and V. Surazhsky. Guaranteed intersection-free polygon morphing. *Computers and Graphics*, 25(1):67–75, 2001.

[25] P. M. Gruber and J. M. Wills, editors. *Handbook of convex geometry*. North-Holland Publishing Co., Amsterdam, 1993.

[26] J. E. Hopcroft and P. J. Kahn. A paradigm for robust geometric algorithms. *Algorithmica*, 7(4):339–380, 1992.

[27] T. Kanai, H. Suzuki, and F. Kimura. Metamorphosis of arbitrary triangular meshes. *IEEE Computer Graphics and Applications*, 20(2):62–75, 2000.

[28] K. Kuratowski. Sur le problème des courbes gauches en topologie. *Fundamenta mathematicae*, 15:271–283, 1930.

[29] B. Lévy and J.-L. Mallet. Non-distorted texture mapping for sheared triangulated meshes. In *SIGGRAPH 1998*, pages 343–352, 1998.

[30] N. Linial, L. Lovász, and A. Wigderson. Rubber bands, convex embeddings and graph connectivity. *Combinatorica*, 8(1):91–102, 1988.

[31] J. Orlin. Line-digraphs, arborescences, and theorems of Tutte and Knuth. *Journal of Combinatorial Theory. Series B*, 25(2):187–198, 1978.

[32] J. Richter-Gebert. *Realization spaces of polytopes*, volume 1643 of *Lecture Notes in Mathematics*. Springer-Verlag, 1996.

[33] O. Schramm. How to cage an egg. *Inventiones mathematicae*, 107:543–560, 1992.

[34] M. Starbird. A complex which cannot be pushed around in E^3. *Proceedings of the American Mathematical Society*, 63(2):363–368, 1977.

[35] M. Starbird. Linear isotopies in E^3. *Proceedings of the American Mathematical Society*, 65(2):342–346, 1977.

[36] M. Starbird. The Alexander linear isotopy theorem in E^3. In *Continua, decompositions, manifolds*, pages 243–267. Univ. Texas Press, Austin, 1983.

[37] S. K. Stein. Convex maps. *Proceedings of the American Mathematical Society*, 2:464–466, 1951.

[38] C. Thomassen. Kuratowski's theorem. *Journal of Graph Theory*, 5(3):225–241, 1981.

[39] C. Thomassen. Deformations of plane graphs. *Journal of Combinatorial Theory, Series B*, 34:244–257, 1983.

[40] W. T. Tutte. How to draw a graph. *Proceedings of the London Mathematical Society*, 13:743–768, 1963.

[41] G. Vegter. Computational topology. In J. E. Goodman and J. O'Rourke, editors, *Handbook of Discrete and Computational Geometry*, chapter 28, pages 517–536. CRC Press LLC, Boca Raton, FL, 1997.

[42] K. Wagner. Bemerkungen zum Vierfarbenproblem. *Jahresbericht der Deutschen Mathematiker-Vereinigung*, 46:26–32, 1936.

[43] W. Whiteley. Motions and stresses of projected polyhedra. *Structural Topology*, 7:13–38, 1982.

[44] D. Zeilberger. A combinatorial approach to matrix algebra. *Discrete Mathematics*, 56(1):61–72, 1985.

[45] G. M. Ziegler. *Lectures on Polytopes*, volume 152 of *Graduate Texts in Mathematics*. Springer-Verlag, 1994.